

Origin of postmaximum bump in luminous type Ic SN 2019stc

Nikolai N. Chugai^{1*} and Victor P. Utrobin^{1,2,3}

¹*Institute of Astronomy, Russian Academy of Sciences, Pyatnitskaya St. 48, 119017 Moscow, Russia*

²*NRC ‘Kurchatov Institute’ – Institute for Theoretical and Experimental Physics, B. Chermushkinskaya St. 25, 117218 Moscow, Russia*

³*Max-Planck-Institut für Astrophysik, Karl-Schwarzschild-Str. 1, 85748 Garching, Germany*

Accepted XXX. Received YYY; in original form ZZZ

ABSTRACT

We address the issue of the postmaximum bump observed in the light curve of some superluminous supernovae. We rule out the popular mechanism of a circumstellar interaction suggested for the bump explanation. Instead we propose that the postmaximum bump is caused by the magnetar dipole field enhancement several months after the explosion. The modeling of SN 2019stc light curve based on the thin shell approximation implies that at the age of ~ 90 days the initial dipole magnetic field should be amplified by a factor of 2.8 to account for the postmaximum bump. The specific mechanism for the field amplification of the newborn magnetar on the timescale of several months has yet to be identified.

Key words: supernovae: general – supernovae: individual: SN 2019stc

1 INTRODUCTION

In the last decade, a new category of supernovae (SNe) has been discovered — hydrogen-free superluminous supernovae (SLSNe-I) with the luminosity $> 3 \times 10^{43}$ erg s⁻¹ (Gal-Yam 2019). Their radiation is presumably powered by a magnetar (Maeda et al. 2007; Kasen & Bildsten 2010; Woosley 2010; Kasen et al. 2016), possibly with some contribution of radioactive ⁵⁶Ni (e.g. Gomez et al. 2021). While a standard magnetar mechanism is able to describe the light curve, including the early brief (< 10 d) bump (Kasen et al. 2016), it cannot account for the postmaximum bump seen in some SLSNe-I 1 – 2 months after the main light maximum, viz. in SN 2019stc (Gomez et al. 2021). The occurrence of the postmaximum bump among SLSNe and its origin have been recently analyzed by Yan et al. (2017) and Hosseinzadeh et al. (2021) with the conclusion that the circumstellar (CS) interaction or the variability of a central engine could be responsible for the bump. At the moment Hosseinzadeh et al. (2021) do not find any evidence to favor one mechanism over another.

As a matter of fact, there is a strong argument against the CS interaction. Indeed, the light curve of SN 2019hge (SLSN-I) demonstrates a clear-cut postmaximum bump similar to that of SN 2019stc, yet SN 2019hge spectra (Yan et al. 2020) show pronounced He I absorption lines through the extended period of time, including the epoch of the postmaximum bump. The presence of He I absorptions at the bump stage means that the bulk of luminosity is generated in the ejecta interior, *and not by the CS interaction*. This implies that the likely reason for the bump origin of SLSNe-I is a variability of a central engine.

Here we propose and explore an alternative conjecture that the postmaximum bump is related to the enhancement of the dipole magnetic field of the magnetar that causes the higher magnetar lu-

minosity responsible for the bump. At the moment, we are not able to identify a specific mechanism for the field enhancement. Yet the conjecture finds an indirect support in the variety of mechanisms for the magnetic field amplification of a newborn neutron star by means of, e.g., convective dynamo (Raynaud et al. 2020), shear-Hall instability (Kondić et al. 2011), precession-driven amplification (Lander 2021), and reconfiguration of a partially submerged magnetic field (Torres-Forné et al. 2016). In the absence of reasonable alternative the effect of the enhancement of the dipole magnetic field should be taken as a viable possibility and must be explored. We will apply our conjecture to the description of the light curve of the recent well-observed luminous type Ic supernova SN 2019stc (Gomez et al. 2021) that shows a conspicuous postmaximum bump.

2 SCENARIO AND MODEL OVERVIEW

We suggest that the explosion of a WR star at ~ 50 d before the light maximum (~ 10 d before the SN discovery) with the energy $E \sim 10^{51}$ erg ejects a freely expanding envelope with the mass $M \sim 10 M_{\odot}$ and the density distribution $\rho = \rho_0(t)/(1 + u^9)$, where $u = v/v_0$, while ρ_0 and v_0 are determined by E and M . A rapidly rotating newborn neutron star loses the rotational energy presumably via the magnetized relativistic wind (Kennel & Coroniti 1984) that inflates the bubble with the energy E_b , the volume V_b , and the relativistic pressure $p \sim (1/3)E_b/V_b$. The bubble expansion sweeps up the gas of the freely expanding envelope into a thin shell. This shell however is liable to the Rayleigh-Taylor (RT) instability that is absent in our model. Yet we take into account the effect of the RT fragmentation of the swept-up shell in the computation of the optical depth assuming homogeneous distribution of the swept-up mass in the bubble. The internal energy of the bubble is spent on the pressure work, and on the escaping radiation responsible for the observed bolometric luminosity.

* E-mail: nchugai@inasan.ru

The issue of the conversion of a relativistic wind, dominated by Poynting flux, into the wind with the significant fraction of the particle thermal energy (e.g. [Coroniti 2017](#)) that powers the light curve is beyond our task. Below we simply admit that some fraction η of the magnetar luminosity L_m goes into the thermal energy in the form of radiation, while the remaining fraction $(1-\eta)$ resides in the magnetic energy. We also admit that the value η can be variable ([Kasen et al. 2016](#)). Both radiation and magnetic energy compose the bubble internal energy $E_b = E_r + E_m$ with the relativistic pressure p assumed to be uniform in the spherical volume V_b .

The magnetar luminosity is determined by the magnetic dipole radiation of the rotating dipole with the angular frequency Ω : $L_m = (2/3)(\mu \sin \chi)^2 \Omega^4 / c^3 = (2/3)B_0^2 R_{ns}^6 \Omega^4 / c^3$, where χ is the angle between the magnetic moment μ and the rotational axis and B_0 is the equatorial component of the surface magnetic field ([Landau & Lifschits 1975](#)). More relevant is the expression for the spin-down losses obtained via magnetohydrodynamic simulations $L_m = \mu^2 \Omega^4 (1 + \sin^2 \chi)^2 / c^3$ ([Philippov et al. 2015](#)). Yet we employ the expression for the magnetic dipole radiation that is widely used for the magnetar in SLSNe-I (e.g. [Chen et al. 2020](#)). This means that the magnetic field estimate can differ from a realistic value by a factor of the order of unity.

The equations of motion, magnetic and radiation energy, and mass conservation in the thin shell approximation with the shell mass M_s , the radius r_s , the velocity v_s , and the undisturbed SN density $\rho(t, r)$ at the radius r_s read

$$M_s \frac{dv_s}{dt} = 4\pi r_s^2 [p - \rho(v_s - \frac{r_s}{t})^2] \quad (1)$$

$$\frac{dE_m}{dt} = -\frac{E_m v_s}{r_s} + (1-\eta)L_m \quad (2)$$

$$\frac{dE_r}{dt} = -\frac{E_r v_s}{r_s} - L_b + \eta L_m \quad (3)$$

$$\frac{dM_s}{dt} = 4\pi r_s^2 \rho (v_s - \frac{r_s}{t}) \quad (4)$$

The luminosity of the radiation escaping from the bubble is $L_b = E_r / t_d$, where t_d is the diffusion time for the bubble photons taken to be equal to the average escape time for the case of a central source in the homogeneous envelope of the radius r and optical depth τ , i.e., $t_d = t_{esc} = (r/c)\tau/2$ (e.g. [Sunyaev & Titarchuk 1980](#)). In our case $r = \max(v_0 t, r_s)$ and τ is the total optical depth of the shell plus external ejecta $\tau = \tau_s + \tau_e$.

The supernova luminosity includes also the radiation produced by the radiative shock driven by the swept up shell. In this respect our model is similar to that of [Kasen et al. \(2016\)](#) and differs from the model by [Gomez et al. \(2021\)](#) that does not include this luminosity component. The shock luminosity is approximated as

$$L_s = 2\pi r_s^2 \rho \left(v_s - \frac{r_s}{t}\right)^3 \frac{t}{(t + t_e)}, \quad (5)$$

where t_e is the diffusion time for the external ejecta $t_e = \max(v_0 t, r_s)\tau_e/2$. The total supernova luminosity is thus $L_{sn} = L_b + L_s$. We include the radioactive ^{56}Ni presumably residing in the deep interior of the ejecta. We use the constant opacity $k = 0.1 \text{ cm}^2 \text{ g}^{-1}$ that is twice as lower compared to the value adopted earlier ([Gomez et al. 2021](#)).

The additional component of the dipole field responsible for the postmaximum bump can be described via a smooth step function $\theta(t)$ and a relative amplitude h with respect to the initial field B_0 as $B_1(t) = hB_0\theta(t)$. The function $\theta(t)$ is specified by the moment of the additional field turn on t_1 and the field rise time t_2 . We find it

Table 1. Model parameters

Parameter	Units	mag8	mag8ni
E	10^{51} erg	0.8	0.8
M	M_\odot	8	8
B_0	10^{13} G	5	5
p_0	10^{-3} s	2.5	2.5
η		0.46	0.43
h		1.8	1.8
M_{Ni}	M_\odot	0	0.2
t_1	days	92	92
t_2	days	25	25
t_m	days	52.5	52
E_f^\dagger	10^{51} erg	3.9	3.9

† Final kinetic energy.

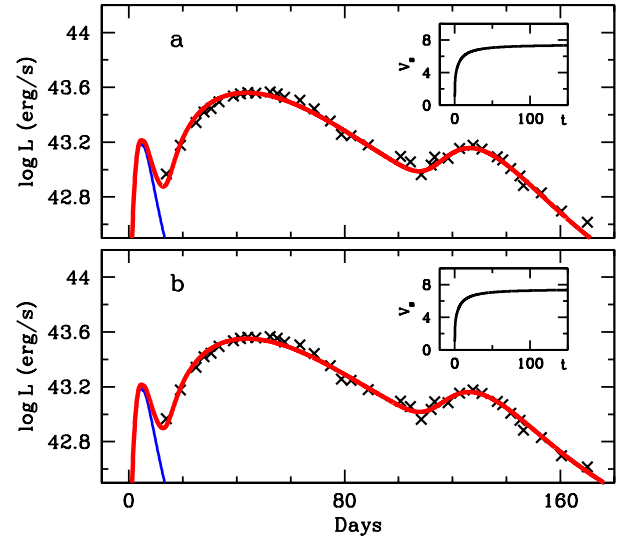


Figure 1. Model bolometric light curve of SN 2019stc (red) overlotted on the observational bolometric light curve (crosses) reported by [Gomez et al. \(2021\)](#). Panels (a) and (b) correspond to models mag8 and mag8ni, respectively (Table 1). Thin blue line shows the contribution of the luminosity of the radiative shock driven by the expanding bubble. Inset demonstrates the evolution of the thin shell speed in units of 1000 km s^{-1} .

convenient to set $\theta(t)$ as

$$\theta(x) = \begin{cases} 0 & \text{if } x < 0 \\ x^4 / (1 + x^4) & \text{if } x \geq 0, \end{cases} \quad (6)$$

where $x = (t - t_1)/t_2$. The overall dipole field is thus $B = B_0[1 + h\theta(x)]$. Values of t_1 , t_2 , and h are recovered from the optimal fit of the light curve.

3 LIGHT CURVE MODEL

The bolometric light curve of SN 2019stc analyzed here is recovered by [Gomez et al. \(2021\)](#). We present two models: model mag8 without radioactive ^{56}Ni and model mag8ni with a maximal amount of ^{56}Ni of $0.2 M_\odot$ (Table 1) consistent with the observational light curve (Fig. 1). The adopted neutron star mass, its radius and moment of inertia are $M_{ns} = 1.4 M_\odot$, $R_{ns} = 12 \text{ km}$, and $I = 1.2 \times 10^{45} \text{ g cm}^2$, respectively. Table 1 contains from top to bottom: the explosion energy, the ejecta mass, the dipole surface magnetic field, the initial

rotation period, the thermalized fraction of the relativistic wind, the relative amplitude of the additional component of the dipole field, the radioactive ^{56}Ni mass, the turn on moment of the field amplification, the rise time of the field, and the time of the light maximum after the explosion. Shown at the bottom is the final kinetic energy of the ejecta that exceeds the explosion energy by the $p dV$ work produced by the magnetar driven bubble. The relative error of parameters of the additional field component t_1 , t_2 , and h is about 5%.

Both models fit the observational light curve fairly well and provide required velocity (7000 km s^{-1}) of the bubble boundary on +15 d after the light maximum. The initial peak of the model light curve is related to the radiative shock driven by the bubble expansion that is absent in the model of Gomez et al. (2021). This shock is identified by Kasen et al. (2016) with the early bump seen in several SLSNe-I. The early bump generally affects the rise of the light towards the main maximum. To describe the light curve of SN 2019stc, one needs to adopt that during the first 12 days the magnetar wind has the low thermalization parameter is low $\eta = 0.053$ with the subsequent transition to the larger value $\eta = 0.46$ and $\eta = 0.43$ in models mag8 and mag8ni, respectively.

Disregarding these details we stress our major result: the postmaximum bump is well reproduced in the model with the initial dipole field of the magnetar $5 \times 10^{13} \text{ G}$ that is enhanced to $1.4 \times 10^{14} \text{ G}$ at about 100 d after the explosion. We believe that the proposed scenario for the origin of the postmaximum bump is applicable to the most of similar cases of SLSNe-I, including SN 2019hge that permits us to abandon the alternative mechanism based on the circumstellar interaction.

Our simple model has an apparent drawback, viz., at the postmaximum stage it predicts that expanding ejecta should contain “empty” bubble with the velocity of $\sim 7000 \text{ km s}^{-1}$. Formally this suggests that the profile of an emission line, e.g., $\text{O I } 7774 \text{ \AA}$ should be flat-topped in the range of $\sim \pm 7000 \text{ km s}^{-1}$, which is not the case (cf. Gomez et al. 2021). In reality, the swept-up shell accelerated by the relativistic bubble is liable to the RT instability (Chevalier & Fransson 1992). This results in a picture of light bubbles penetrating the ejecta along with spikes of a dense shell material trailed behind (e.g. Layzer 1955). The spikes are subject to the stripping due to a shear flow, so the expanding relativistic bubble turns out filled by the ejecta material as demonstrates by 3D-simulation (Chen et al. 2020). These 3D-hydrodynamic effects thus should resolve the issue of the bubble emptiness of our one-dimensional model.

4 CONCLUSION

We found strong argument against the CS interaction as a mechanism for the bump emergence, which means that the only viable possibility is the variability of the central engine. We explored the proposed conjecture that the postmaximum bump of the SN 2019stc bolometric light curve is related to the magnetar dipole field increase at about three months after the explosion. The modeling suggests that the postmaximum bump is reproduced, if the dipole magnetic field is increased by a factor of ~ 2.8 on the time scale of $\sim 25 \text{ d}$ starting from day 92 after the explosion.

The physics behind the significant field amplification in three months after the core collapse has yet to be identified. Presumably it could be related to mechanisms mentioned in the Introduction: either the convective field amplification or the reconfiguration of a partially submerged magnetic field.

ACKNOWLEDGEMENTS

We thank Maxim Barkov for discussions on a newborn magnetar field transformation. The reported study was funded by RFBR and DFG, project number 21-52-12032.

DATA AVAILABILITY

The data underlying this article will be shared on reasonable request to the corresponding author.

REFERENCES

- Chen K.-J., Woosley S. E., Whalen D. J., 2020, *ApJ*, **893**, 99
 Chevalier R. A., Fransson C., 1992, *ApJ*, **395**, 540
 Coroniti F. V., 2017, *ApJ*, **850**, 184
 Gal-Yam A., 2019, *ARA&A*, **57**, 305
 Gomez S., Berger E., Hosseinzadeh G., Blanchard P. K., Nicholl M., Villar V. A., 2021, *ApJ*, **913**, 143
 Hosseinzadeh G., Berger E., Metzger B. D., Gomez S., Nicholl M., Blanchard P., 2021, arXiv e-prints, p. arXiv:2109.09743
 Kasen D., Bildsten L., 2010, *ApJ*, **717**, 245
 Kasen D., Metzger B. D., Bildsten L., 2016, *ApJ*, **821**, 36
 Kennel C. F., Coroniti F. V., 1984, *ApJ*, **283**, 694
 Kondić T., Rüdiger G., Hollerbach R., 2011, *A&A*, **535**, L2
 Landau L. D., Lifschits E. M., 1975, *The Classical Theory of Fields. Course of Theoretical Physics Vol. Volume 2*, Pergamon Press, Oxford
 Lander S. K., 2021, *MNRAS*, **507**, L36
 Layzer D., 1955, *ApJ*, **122**, 1
 Maeda K., et al., 2007, *ApJ*, **666**, 1069
 Philippov A. A., Spitkovsky A., Cerutti B., 2015, *ApJ*, **801**, L19
 Raynaud R., Guilet J., Janka H.-T., Gastine T., 2020, *Science Advances*, **6**, eaay2732
 Sunyaev R. A., Titarchuk L. G., 1980, *A&A*, **500**, 167
 Torres-Forné A., Cerdá-Durán P., Pons J. A., Font J. A., 2016, *MNRAS*, **456**, 3813
 Woosley S. E., 2010, *ApJ*, **719**, L204
 Yan L., et al., 2017, *ApJ*, **848**, 6
 Yan L., et al., 2020, *ApJ*, **902**, L8

This paper has been typeset from a $\text{\TeX}/\text{\LaTeX}$ file prepared by the author.